

**Figure 4.** Gel curve  $h(E)$  and derived exposure function  $Y(E)$  of polymer III exposed to monochromatic radiation of 350 nm.

gained from repeat measurements on polymer II carried out in other laboratories: A light scattering experiment at the National Physical Laboratory in Teddington gave  $M_w = 5.2 \times 10^4$  (compared with our value of  $4.9 \times 10^4$ ), and a determination of  $M_n$  by membrane osmometry (solvent, toluene) at Liverpool University gave  $M_n = 1.1 \times 10^4$ , which together with the ratio  $M_w/M_n = 4.3$  obtained by gel permeation chromatography at Imperial College, London (compared with a value of 4.2 found in this laboratory), leads to a value of  $M_w = 4.73 \times 10^4$ . These data reflect an uncertainty of less than  $\pm 5\%$  in the determination of  $M_w$  and lead, for  $\Phi$ , to the error limits indicated in Table II.

The determination of the overall quantum yield  $\phi$  is more straightforward; however, it involves the gradient of a directly measured quantity ( $dD/dt$ ), and its accuracy is therefore not higher than  $\pm 8\%$ .

It can be seen from the data in Table II that within the accuracy of the experiment the quantum yield of intermolecular cross-link formation is identical with the overall quantum yield of the cross-link forming reaction: in polymers I, II, and III the formation of intramolecular cross-links, or loops, appears to be negligible. This indicates a high degree of coil interpenetration in the solid matrices of the polymers, in agreement with results of recent neutron scattering experiments,<sup>9</sup> and also in accord

with the strongly held views of Flory.<sup>20,21</sup>

**Acknowledgment.** We are grateful to Mr. R. C. McConkey (Eastman Kodak) for the preparation of polyester II, to Dr. John Reddington and Mrs. Sheila O'Keeffe (Kodak Limited) and Dr. R. Dietz (National Physical Laboratory) for the molecular weight determinations, to Dr. Martyn Lambert (Kodak Limited) and Dr. D. J. Walsh (Imperial College, London) for the gel permeation chromatography, and to Professor C. H. Bamford F.R.S. (Liverpool University) for the osmometric result.

## References and Notes

- (1) P. J. Flory, "Statistical Mechanics of Chain Molecules", Interscience, New York, 1969.
- (2) A. J. Chomppf and S. Newman, Eds., "Polymer Networks, Structure and Mechanical Properties", Plenum Press, New York, 1971.
- (3) D. Braun, *Angew. Chem., Int. Ed. Engl.*, **15**, 451 (1976).
- (4) R. F. Boyer in "Physical Structure of the Amorphous State", G. Allen and S. E. B. Petrie, Eds., Marcel Dekker, New York, 1976, p 253.
- (5) W. W. Graessley, *Adv. Polym. Sci.*, **16**, 1 (1974).
- (6) W. R. Krigbaum and R. W. Godwin, *J. Chem. Phys.*, **43**, 4523 (1965).
- (7) Hyo-Gun Kim, *J. Appl. Polym. Sci.*, **22**, 889 (1978).
- (8) D. G. H. Ballard, J. Schelten, and G. D. Wignall, *Eur. Polym. J.*, **9**, 965 (1973).
- (9) A. Maconnachie and R. W. Richards, *Polymer*, **19**, 739 (1978), and references therein.
- (10) S. M. Aharoni, *Macromolecules*, **11**, 677 (1978).
- (11) B. Vollmert and H. Stutz, *Angew. Makromol. Chem.*, **20**, 71 (1971).
- (12) B. Vollmert and H. Stutz, *Angew. Makromol. Chem.*, **35**, 75 (1973).
- (13) (a) D. Braun and F. J. Quesada Lucas, *Makromol. Chem.*, **142**, 313 (1971); (b) S. M. Aharoni, *Angew. Makromol. Chem.*, **62**, 115 (1977).
- (14) F. I. Sonntag and R. Srinivasan, *Tech. Pap., Reg. Tech. Conf., Soc. Plast. Eng., Mid-Hudson Sect.*, 163–170 (1967).
- (15) A. Reiser and P. L. Egerton, *Photogr. Sci. Eng.*, to be published.
- (16) W. H. Stockmayer, *J. Chem. Phys.*, **12**, 125 (1944).
- (17) P. J. Flory, "Principles of Polymer Chemistry", Cornell University Press, Ithaca, N.Y., 1953, p 380.
- (18) N. J. H. Parham, E. Pitts, and A. Reiser, *Photogr. Sci. Eng.*, **21**, 145 (1977).
- (19) Farbenfabriken Bayer A.G., British Patent 838 547 (1968).
- (20) P. J. Flory, *Macromol. Chem.*, **8**, 1 (1973).
- (21) P. J. Flory in "Physical Structure of the Amorphous State", G. Allen and S. E. B. Petrie, Eds., Marcel Dekker, New York, 1976, pp 1–11.
- (22) The integration assumes a constant quantum yield of cross-link formation. This is justified in our experiments, since the overall degree of chromophore conversion in the polymer films is low (2–3%).

## Properties of Networks Formed by End Linking of Poly(dimethylsiloxane)

Enrique M. Valles<sup>1</sup> and Christopher W. Macosko\*

Department of Chemical Engineering and Materials Science, University of Minnesota, Minneapolis, Minnesota 55455. Received May 17, 1978

**ABSTRACT:** Networks with well-defined structures were prepared by end linking vinyl-terminated poly(dimethylsiloxane) chains with tri- and tetrafunctional silanes. Modulus and extent of reaction were followed continuously on several systems. If trapped entanglements are accounted for, the modulus rise can be modeled quantitatively with branching theory. The effect of entanglements is demonstrated by changing molecular weight of the chains and by dilution. Comparison of data between tri- and tetrafunctional cross-linkers indicates clearly the importance of junction mobility. The  $C_2$  Mooney–Rivlin constant is small. Sol fraction and swelling data are also in reasonable agreement with predictions from branching theory.

Most structural information on networks is inferred from some type of elasticity measurement such as swelling or tensile modulus. It is hoped that such data interpreted

through rubber elasticity theory will give an accurate measure of the average molecular weight between chemical junctions in the network. With this value and supporting

measurements such as fraction of soluble material, the efficiency of cross-linking chemistry can be determined. This in turn can be used to build a structural understanding of performance properties such as stress-strain response, failure, mechanical damping, permeability, and environmental stability.

A major problem in this approach is that there are still discrepancies in the literature as to the correct formulation of the rubber elasticity theory on a molecular basis. The chief problem that has plagued experimental verification of the molecular aspects of the theory is uncertainty in network structure. We have recently described a chemical cross-linking system, the end linking of vinyl terminated poly(dimethylsiloxane) chains with multifunctional silanes, which gives networks of well-defined topology.<sup>2-5</sup> This paper summarizes our earlier studies with these networks, presents new results, and compares these results to those of the classical theory of rubber elasticity and some recent modification to it. First we review the theories and then describe our measurements.

### Review of Theory

For a perfectly elastic material the work done by a deformation is just the change in free energy

$$\mathbf{T} = dW/d\mathbf{B} \quad (1)$$

Here  $\mathbf{T}$  is the stress tensor,  $\mathbf{B}$  is the Finger measure of deformation, and  $W$  is the free energy of deformation per unit volume. Rivlin<sup>6</sup> showed that for an isotropic, incompressible, elastic material the free energy can only be a function of the first and second invariants of the deformation tensor,  $I_B$  and  $II_B$ . This leads to the general constitutive relation

$$\mathbf{T} = -p\mathbf{I} + 2 \frac{\partial W}{\partial I_B} \mathbf{B} - 2 \frac{\partial W}{\partial II_B} \mathbf{B}^{-1} \quad (2)$$

where  $p$  is an arbitrary hydrostatic pressure and  $\mathbf{I}$  is the identity matrix.

Rubber networks can be made homogeneous and are essentially incompressible. Thus eq 2 can be used to predict the equilibrium stresses in a rubber sample for any particular deformation such as simple tension or shear. The key to relating elastic response to molecular structure is determining the free energy from the network topology. This is done through the classical theory of rubber elasticity.<sup>7-10</sup>

**The Phantom Network.** Rubber elasticity theory assumes that a network is made up of random coil strands connected at junction points. The free energy,  $W$ , can be calculated for a single random coil from the reduction in possible configurations as the ends of the coil are displaced. In the classical theory, the strands can fluctuate, i.e., change configuration continuously due to Brownian motion, as if they were in a  $\Theta$  solvent. It is assumed that there is no interference from neighboring chains; i.e., the chains can pass through each other like phantoms. With these assumptions,  $W$  for a single chain becomes

$$W_i = kT \left( \frac{I_B}{2} - \frac{3}{2} \right) \quad (3)$$

There has been considerable discussion in the literature as to how to correctly sum up all the individual chains to obtain  $W$  for the entire network. Many authors have argued that all the ends of the chain move affinely, that is with the macroscopic deformation. With this assumption, the total free energy is just the summation of all the individual strands

$$W = \nu kT \left( \frac{I_B}{2} - \frac{3}{2} \right) \quad (4)$$

where  $\nu$  is the number of network strands per unit volume.

However, recently Graessley<sup>11,12</sup> and Flory<sup>13</sup> have shown that the chain junctions will only move affinely if they have very high functionality. For typical elastomers, junction functionality is 3 or 4 so that the mobility or fluctuation of the junctions must also be considered. They show that junction fluctuation decreases the free energy change with deformation by the concentration of junctions per unit volume of the network  $\mu$ . Thus for a phantom network

$$W = (\nu - \mu)kT \left( \frac{I_B}{2} - \frac{3}{2} \right) \quad (5)$$

If the network is perfect, no dangling chains, and made of tetrafunctional junctions, there will be two strands for every junction and  $\nu - \mu = 1/2\nu$ . However, most networks are not perfect and often have a mixture of junction functionality. Miller and Macosko<sup>14</sup> show how to calculate  $\nu$  and  $\mu$ , particularly for networks formed by end-linking chains as a function of extent of reaction and cross-linker type. Some of these relations are given in the Appendix. Similar relations for random cross-linking of long chains are also available.<sup>12</sup>

If eq 5 for  $W$  is substituted into eq 2, we obtain the constitutive equation for a network of noninteracting strands

$$\mathbf{T} = -p\mathbf{I} + (\nu - \mu)kT\mathbf{B} \quad (6)$$

This equation can be used to calculate stress-strain relations in all the common experimental test methods.<sup>6,8</sup> For example, in simple shear

$$\tau = T_{12} = (\nu - \mu)kT\gamma \quad (7)$$

where  $\gamma = B_{12}$  is the shear strain. The shear modulus,  $G$ , is a convenient way to express the molecular structure parameters

$$G = \tau/\gamma = (\nu - \mu)kT \quad (8)$$

In simple extension or compression

$$\sigma = T_{11} - T_{22} = G(\lambda^2 - 1/\lambda) \quad (9)$$

where  $\sigma$  is the true stress on the ends of the sample and  $\lambda$  is the extension ratio, stretched length divided by original length.<sup>6,8</sup> In the limit of small extensions, the tensile modulus is just

$$\lim_{\lambda \rightarrow 1} \frac{\sigma}{\lambda - 1} = E = 3G \quad (10)$$

This then is the attractiveness of the rubber elasticity theory. From a few reasonable assumptions about a network, a very simple elasticity relation can be developed. Qualitatively it has compared well to mechanical measurements, but there is quantitative disagreement particularly at large tensile strains. Also some recent studies at small strains have shown that the shear modulus is much higher than predicted by eq 8 (e.g., ref 3-5, 10, and 15-19).

**Entanglements.** The major source of these deviations seems to be chain-chain interactions usually termed entanglements. The basic argument is that the chains in fact are not phantom-like and cannot pass through each other. At small strains, these entanglements can raise the modulus considerably. Under large amounts of tension, these interactions are not as effective, and the modulus appears to decrease. At present there is no firm molecular model

for the effect of entanglements on network elasticity. A number of approaches have been suggested.

The earliest and still the most common treatment for the large tensile strain data is the empirical Mooney–Rivlin equation, based on the general elastic constitutive equation, eq 2. Note that the phantom network model, eq 6, is the simplest case of eq 2, where  $\partial W/\partial I_B = \text{constant} = (\nu - \mu)kT$  and  $\partial W/\partial II_B = 0$ . Mooney found that including  $\partial W/\partial II_B$  as a second constant,  $C_2$ , gave a better fitting of large strain tensile data. For tension/compression the Mooney–Rivlin equation reduces to

$$\sigma = (2C_1 + 2C_2/\lambda)(\lambda^2 - 1/\lambda) \quad (11a)$$

or in terms of  $f$ , the tensile force divided by the original cross-sectional area

$$f = (2C_1 + 2C_2/\lambda)(\lambda - 1/\lambda^2) \quad (11b)$$

Although this relation does not fit compression and biaxial extension data very well, the  $C_2$  term has been widely interpreted on a molecular basis to attempt to understand departures from the phantom network theory.<sup>20</sup>

There have been many other phenomenological equations but few on a molecular basis.<sup>8,10</sup> Recently, Flory has proposed that all chain–chain interactions can be expressed as a suppression of junction fluctuations but that these interactions become less effective under tensile strain.<sup>13,21</sup> This leads to a strain energy function which goes from eq 4 at small strain to eq 5 at large strain. It gives a shape closer to actual tension/compression data than the Mooney–Rivlin equation; however, Flory's model predicts that the small strain modulus is simply the earlier affine chain result (eq 4).

$$G = \nu kT \quad (12)$$

This does not allow for differences in chain–chain interactions between different types of polymers which seem in fact to occur.

Langley<sup>16,22</sup> has proposed a small strain relation which does allow for differences in entanglement contribution between polymers. Langley noted that when a high molecular weight linear polymer is tested under dynamic conditions, the modulus remains roughly constant over a wide range of time or frequency. If molecular weight is increased, the time span of the rubbery plateau increases, but the level remains constant.<sup>15</sup> This plateau is usually explained as being due to a network of entanglements which cannot relax out in the time scale of the measurements. Many authors have argued that cross-linking a polymer could permanently trap part of this entanglement network. Langley proposed that the experimental small strain modulus is just the addition of the phantom and entanglement networks

$$G = (\nu - \mu)kT + T_e G_e \quad (13)$$

where  $T_e$  is a trapping factor and  $G_e$  is the maximum contribution to the modulus due to trapped entanglements. It is expected that  $G_e$  should be close to  $G_N^0$ , the modulus of the rubbery plateau from experiments on linear chains. Langley,<sup>22</sup> Miller and Macosko,<sup>14</sup> and Pearson and Graessley<sup>12</sup> show how to calculate  $T_e$  for various type networks. For a perfect network, there should be no dangling chains,  $T_e = 1$ . It should be noted that eq 13 is only a small strain model. It cannot be used, in this form, to understand the large strain deviations, whereas Flory's approach gives a complete strain energy function.

Below we present results for model silicone networks and compare them to these constitutive relations, particularly eq 8, 12, and 13 at small strains and eq 11 at large strains.

## Experimental Section

Networks were formed by end linking of vinyl terminated poly(dimethylsiloxane) chains, Vi-PDMS, with tri- and tetrafunctional silanes. A platinum complex was used to catalyze the hydrosilation. Two different length Vi-PDMS chains were used,  $M_n = 11\,600$  and  $33\,400$ . The  $11\,600$  was found to contain 5% low molecular weight species by GPC. The reactants, polymerization details, and infrared method for the following extent of reaction are given in ref 2. As in that study, our basic approach here was to follow both extent of reaction and modulus continuously during polymerization on parallel samples from the same mixture, held at the same temperature.

The dynamic shear moduli were monitored by polymerizing the reactants between eccentric rotating disks (ERD) in a Rheometrics mechanical spectrometer.<sup>23</sup> Disks of 2.5-cm diameter were used with 0.01 cm of lateral displacement, a gap of 0.4 cm, and a rotation rate of 1 rad/s. After the reactants were mixed with a mechanical stirrer, they were placed while still liquid between the plates. To hold the sample in position, a sliding plastic cup was placed around the lower disk. This cup was lowered after the gel point was attained.

When the cure reached a level where the storage component of the dynamic modulus,  $G'$ , was greater than  $5 \times 10^4$  N/m<sup>2</sup>, the loss component,  $G''$ , was found to be less than 2% of  $G'$ . This can be seen in Figure 4 where some  $G''$  values are plotted. On the other runs,  $G''$  was even smaller. Thus through most of the cure  $G'$  is expected to be equivalent to the equilibrium modulus  $G$  (ref 24, p 259). This was also verified experimentally by studying the frequency dependence of the modulus. Within experimental error,  $G'$  remained constant with a variation of frequency from  $10^{-3}$  to  $10^2$  rad/s.<sup>5</sup> On fully cured samples,  $G'$  was equal to the equilibrium shear modulus  $G$ , determined by small displacement of one disk without rotation in the mechanical spectrometer.

The elastic component of the modulus was also followed by applying sinusoidal oscillations to samples placed in the cone and plate geometry. Cones of 0.04 and 0.10 rad and 50-mm diameter were used with dynamic strain  $\leq 10\%$  and frequency 1 rad/s. This method was more suitable to detect the onset of gelation.<sup>2</sup> The results for  $G'$  obtained from both methods were in good agreement.

For the tensile measurements, rectangular sheets were prepared by filling several molds of  $1.0 \times 7.0 \times 0.1$  cm with samples of the  $A_3 + B_2$  and  $A_4 + B_2$  systems and letting them react for 96 h at 70 °C to assure complete reaction. The molds were sealed in aluminum foil to avoid contamination.

Samples were stressed at 25 °C by hanging different weights in increasing and decreasing sequences. No creep was observed even during the first few seconds after loading. Elongation was measured with a cathetometer between two marks 3 cm apart.

To determine the fraction of solubles on the different samples, uncross-linked polymer was removed by extraction for 5 days at room temperature in jars with toluene. The solvent was replaced every day. After extraction, the samples were deswollen by placing them in a series of five acetonitrile–toluene mixtures of increasing acetonitrile content and dried in air for 24 h. After the sol content was determined, the strips were swollen in benzene for 2 days, and the degree of swelling was measured by standard techniques.<sup>25</sup> A check of these samples for SiH groups by infrared indicated at least 97% reaction.

## Results and Discussion

Before attempting to compare the various rubber elasticity relations to our results, it is important to verify that our infrared method can in fact accurately measure the extent of reaction and that the assumptions required to apply branching theory to predict the network structure are valid, i.e., equal and independent reactivity and no small loop formation. A number of previous attempts to prepare model networks have not made independent checks of network structure.

Our previous measurements of molecular weight and gel point on this hydrosilation system show that both the infrared method and the branching theory assumptions are very good at least in the pregel region.<sup>2</sup> The weight fraction solubles,  $w_s$ , data given in Table I are a test of the

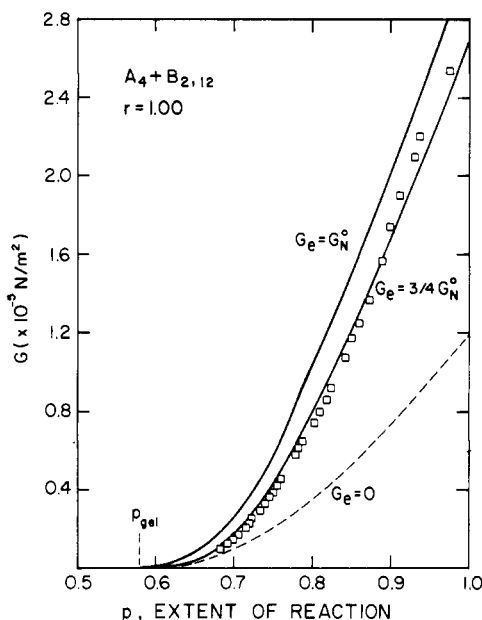


**Figure 1.** Modulus vs. extent of reaction for  $A_4 + B_2$  with  $r = 1.00$ ;  $M_{n,B_2} = 11600$  310 K. Points are from experimental dynamic modulus vs. time and infrared measurements of  $p$  vs. time. The dashed line is from eq 8. The solid lines are from eq 13 with two  $G_e$  values.

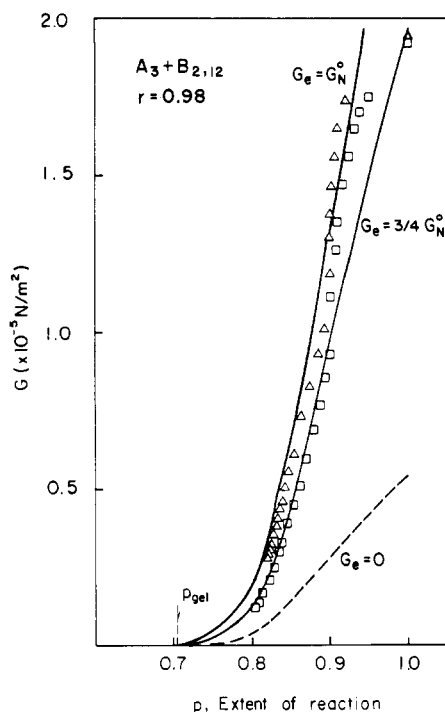


**Figure 2.** Modulus vs. extent of reaction for the  $A_3 + B_2$  system. Same conditions as Figure 1. Triangles and squares correspond to two different runs.

postgel region. With the  $w_s$  data, eq A3 can be used to determine the extent of reaction,  $p$ . We see that for 6 of the 10 samples conversion is 97% or better, in agreement with the infrared. This indicates that the polymerization goes nearly to completion, without side reactions. However, four of the samples show lower conversion, 92–94%. It is important to note that a small measurement error in  $w_s$  for  $r > 1$  leads to large errors in the calculation of  $p$ . For example, for  $r = 1.15$  in the  $A_4 + B_2$  network, 1% sol fraction means an 8% change in conversion. The fact that we had to correct for 5% low molecular weight species in the starting  $B_2$  material means that the small

**Table I**  
Fraction of Soluble Material

	$r^d$	$w_s$ exptl <sup>a</sup>	$w_s$ calcd <sup>b</sup>	$p^c$
$A_3 + B_2$	0.907	0.055	0.011	0.923
	0.960	0.016	0.002	0.940
	0.977	0.010	0.001	0.944
	0.983	0.000	0.000	1.000
	1.009	(-0.004)	0.000	(1.000)
$A_4 + B_2$	0.516	0.347	0.348	1.000
	0.712	0.110	0.095	0.971
	1.150	0.010	0.000	0.920
	1.560	0.013	0.004	0.973
	1.560	0.014	0.004	0.970

<sup>a</sup> Corrected for 5.0% low molecular weight material in the starting  $B_2$ . <sup>b</sup> Using eq A3 with  $p = p_A = 1.0$  for  $r < 1$  and  $p_B = 1.0$ ,  $p_A = 1/r$  for  $r > 1$ . <sup>c</sup> Using eq A3 with experimental  $w_s$  and  $r$  values. <sup>d</sup> Stoichiometric balance.

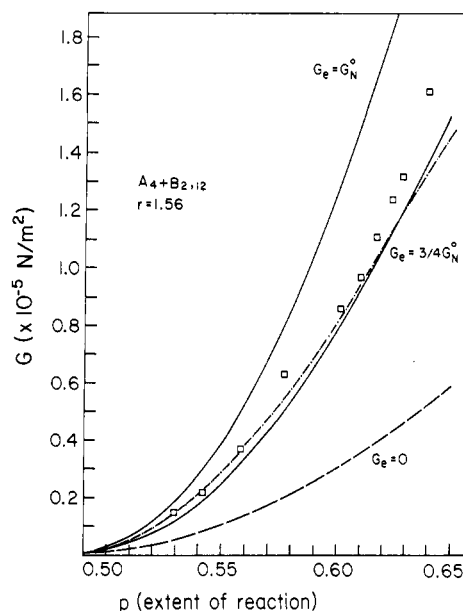


**Figure 3.** Modulus vs. extent of reaction for  $A_4 + B_2$  with  $r = 1.56$ : (---) eq 8; (---) eq 12, (—) eq 13 with two  $G_e$  values.

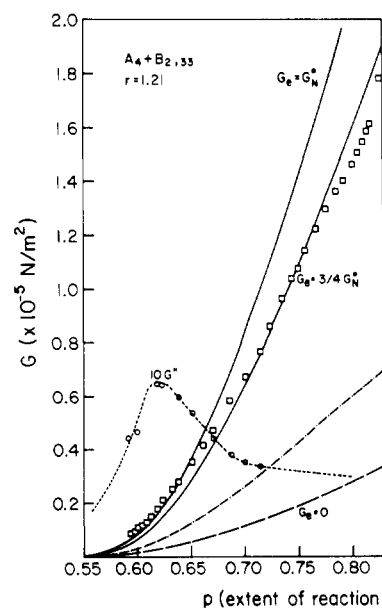


**Figure 4.** Modulus vs. extent of reaction for  $A_4 + B_2$  with  $M_{n,B_2} = 33400$ . Circles correspond to  $G''$  data plotted on a scale ten times that for the  $G'$  data (squares). Theoretical lines are the same as those in Figure 3.

Table II  
PDMS Large Strain Data

network type	$r^a$	$G_{\text{exptl}} \times 10^5 \text{ Pa}$	$G_{\text{calcd}} \times 10^5 \text{ Pa}$	$2C_2 \times 10^5 \text{ Pa}$	$T_e G_e \times 10^5 \text{ Pa}$	$C_2/C_1$
$A_3 + B_2$	1.00	2.59	2.64	0.30	1.56	0.117
$A_3 + B_2$	0.997	2.19	2.25	0.20	1.50	0.102
$A_4 + B_2$	0.740	0.97	0.82	0.36	0.53	0.371
$A_3 + B_2$	0.771	0.57	0.57	0.11	0.29	0.188

<sup>a</sup> Stoichiometric imbalance.

$w_s$  values will be less accurate.

The modulus vs. extent of reaction results are given in Figures 1–4. The experimental  $G'$  vs.  $p$  data appear as points. The two sets of points in Figure 2 indicate reproducibility of duplicate runs. The data are available in tabular form.<sup>5</sup> The lines are predictions of the various theoretical approaches.

In each case we see that the phantom network, eq 8 or 13 with  $G_e = 0$ , underestimates the modulus considerably. Langley's approach, eq 13, comes closer but is consistently higher. Here we have assumed  $G_e$  and  $G_N^0$  and take  $G_N^0 = 2.11 \times 10^5 \text{ N/m}^2$  as measured on linear poly(dimethylsiloxane) in our laboratory.<sup>26</sup> This is in reasonable agreement with literature<sup>27,28</sup> values of  $2.0$  and  $2.99 \times 10^5$ .

If we assume that  $G_e = \frac{3}{4}G_N^0$ , i.e., that the trapped entanglements are somewhat less effective than those causing the plateau modulus, then we have good agreement between eq 13 and the experiments in Figures 1 through 4. The comparison of Figures 1 and 2 is particularly significant. Here all conditions are essentially the same except for the functionality of the cross-linker. This indicates that use of  $(\nu - \mu)$  to account for the higher mobility of the three functional junctions is correct.<sup>11,13</sup>

Flory's approach gives eq 12 for small strains and fits the data of Figures 1 to 3 about as well as eq 13 with  $G_e = \frac{3}{4}G_N^0$ . The fit is indicated in Figure 3. However, in Figure 4 we have results for much larger starting  $B_2$  chains. With so few chemical cross-links, the influence of the trapped entanglements is an even greater fraction of the total modulus.

Figure 4 also shows loss modulus data plotted vs. extent of reaction. We note that  $G''$  is considerably smaller than  $G'$ , even for this network with long chains, and that  $G''$  goes through a maximum at  $p = 0.62$ . We feel that long pendant or dangling chains may be responsible for most of the viscous loss in a network. This is supported by calculation of the weight fraction of pendant chains, eq A9. For the polymerization of Figure 4, the weight fraction of pendant chains also has a maximum at  $p = 0.62$  but a somewhat broader peak.

Although cross-linking in the presence of solvent can increase the number of small loops in the network, for our system, with such long  $B_2$  chains, small amounts of a  $\theta$  solvent should not affect the number of chemical junctions significantly. However, it is well established that  $G_N^0$  is strongly dependent on solvent concentration. A 2.0–2.3 power dependence on concentration has been reported for various linear polymers,<sup>15,24,30</sup> but there appears to be no data specifically on the  $\nu_2$  dependence of  $G_N^0$  for PDMS in the literature.

Figure 5 shows data for an  $A_3 + B_2$  system cross-linked with 14% of a nonreactive low molecular weight PDMS fluid (Dow Corning 200, 1 P). This solvent clearly reduces the  $G$  vs.  $p$  data when compared to Figure 1. Equation 13 with  $G_e = \frac{3}{4}\nu_2^2 G_N^0$  lies somewhat above the data. A better fit is obtained with  $0.55\nu_2^2 G_N^0$  or with  $\frac{3}{4}\nu_2^4 G_N^0$ . Thus our results indicate a stronger dependence on solvent concentration than expected from the data reported for linear chains. Other concentrations should be studied to

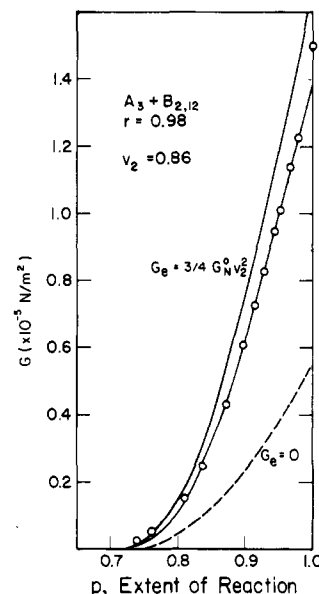


Figure 5. Modulus vs.  $p$  for  $A_3 + B_2$  with 14 wt % diluent, 307 K.

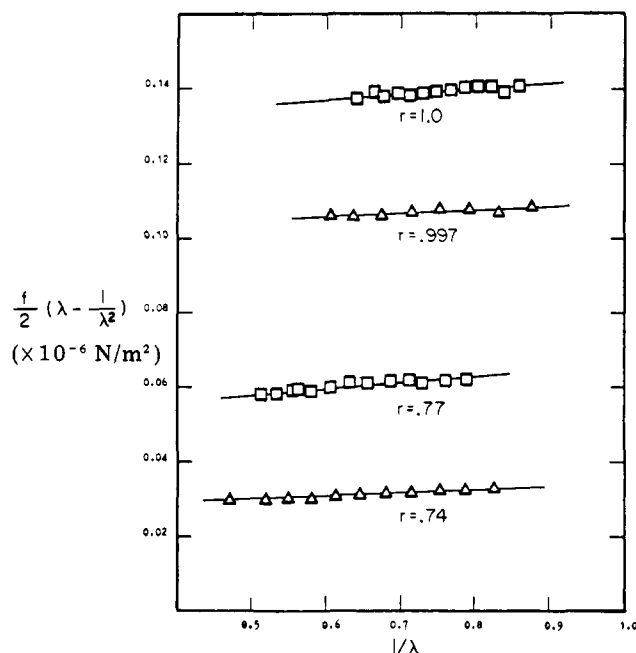


Figure 6. Mooney–Rivlin plot of samples from Table II: (□)  $A_4 + B_2$ , (Δ)  $A_3 + B_2$ .

test this observation further. Dossin<sup>19</sup> finds good agreement with  $\nu_2^2 G_N^0$  for polybutadiene networks with  $\nu_2 = 0.50$ .

We tested several of our network samples at large tensile strain. Plots of eq 11b are shown in Figure 6, and the  $C_1$  and  $C_2$  values evaluated from it are given in Table II. Again on these four samples we see good agreement between the small strain modulus and  $(\nu - \mu)RT + \frac{3}{4}G_N^0 T_e$  (eq 13). A number of studies have suggested that  $C_2$  is

Table III  
Equilibrium Swelling Measurements

	<i>r</i>	<i>v</i> <sub>2</sub>	<i>χ</i> <sub>1</sub> <sup>a</sup>	<i>(ν - μ)</i> , mol/m <sup>3</sup>		<i>c</i>
				exptl <sup>b</sup>	calcd	
A <sub>3</sub> + B <sub>2</sub>	0.960	0.233	0.544	66.9	20.7	69.4
	0.960	0.238	0.547	68.9	20.7	69.4
	0.980	0.243	0.549	72.4	22.7	76.2
	1.009	0.255	0.553	82.7	25.8	86.6
	1.560	0.210	0.539	47.3	15.5	53.4
	1.560	0.219	0.541	53.8	15.5	53.4
	1.150	0.272	0.562	88.2	22.2	78.9
	1.150	0.274	0.563	89.5	22.2	78.9

<sup>a</sup> Reference 31. <sup>b</sup> Equation 14. <sup>c</sup>  $(\nu - \mu) + (3T_e G_N^0/4RT)$  calcd.

some function of the trapped entanglements. Dossin and Graessley<sup>19</sup> find  $2C_2 \approx 1/2 T_e G_e$  fits their data, and Ferry and Kan<sup>32</sup> report a similar relation. We see that the last two samples in Table II, networks with a considerable number of dangling ends, roughly fit this relation. However, the first two samples, nearly completely end-linked networks, show very low  $C_2$  values.

On several of the networks which were used for sol fraction determinations, equilibrium swelling measurements were also made, Table III. Flory's swelling relation (ref 7, p 579), derived from the phantom network, was used to evaluate  $\nu - \mu$

$$\nu - \mu = \frac{\ln(1 - v_2) + v_2 + v_2^2 \chi_1}{V_1 \left( \frac{\mu}{\nu} v_2 - v_2^{1/3} \right)} \quad (14)$$

where  $V_1$  is the molar volume of benzene, and  $\chi_1$  is the polymer solvent interaction parameter. For our calculations,  $\chi_1$  was obtained as a function of volume fraction polymer from the work of Flory and Tatara.<sup>31</sup> The  $\mu/\nu$  term is usually reported as 1/2 which is only valid for tetrafunctional junctions.

The data in Table III again indicate a strong influence of entanglements. As with the shear modulus data, the phantom network can only account for 1/4 to 1/3 the observed number of effective network chains. Using Langley's approach to bring in the contribution of entanglements with  $3/4 G_N^0$  gives much better agreement with experiment. We should note that swelling is a large strain deformation, and we would not necessarily expect such good agreement with Langley's small strain relation. We also note that all the samples studied here lie in a narrow swelling range and thus are not a very definitive test of eq 14.

## Conclusions

A number of conclusions can be drawn from these results.

The end linking of Vi-PDMS with polyfunctional hydrosilanes appears to yield networks of known structure. This is verified by the agreement between the predictions of branching theory and measurements of  $M_w$ , gel point,<sup>2</sup> and sol fraction. However, there is some uncertainty in the  $w_s$  data due to the presence of low molecular weight species in the starting B<sub>2</sub> material. The influence of these species on the mechanical properties of the networks is not known at this time. In future work, such species should be removed before cross-linking.

Permanently trapped chain interactions make a substantial contribution to the modulus and swelling behavior of silicone networks. This contribution appears to be about 3/4 of the plateau modulus,  $G_N^0$ , measured on linear PDMS chains in transient tests.

The predictions of the phantom network theory for the chemical contribution to these silicone networks appear to be correct. In particular, the effect of junction fluctuation is clearly evidenced when the modulus data of tri- and tetrafunctional networks made from the same B<sub>2</sub> chains, Figures 1 and 2 and Table III, are compared.

Departure from the phantom network theory at large tensile strains, eq 9 with  $G$  from eq 13, is small. For completely end-linked silicone networks, the  $C_2$  term of the Mooney-Rivlin equation is about 10% of  $\bar{C}_1$ ; typical elastomers are 50 to 100%. A molecular explanation of the deviation from the phantom theory is not clear from our limited data. Further large strain studies are in progress.

**Acknowledgment.** This work was partially supported by the Army Research Office, the Dow Corning Corp., and the National Research Council of Argentina (CONICET). We are grateful for helpful discussions with Drs. Moshe Gottlieb, William Graessley, and Neal Langley.

## Appendix. Network Parameters

Miller and Macosko<sup>14</sup> have used branching theory to derive equations describing the structure of networks formed by the copolymerization of A<sub>f</sub> with B<sub>2</sub>. They assume an ideal network polymerization: no small loops are formed and all functional groups are equally reactive with the same reactivity throughout the polymerization. Our hydrosilation system obeys these assumptions.<sup>2</sup> Below we give the relations from Miller and Macosko which were used to calculate network properties in this paper.

The fundamental parameter for postgel branching relations is the probability that looking "out" from a functional group leads to a finite chain,  $P(F_A^{\text{out}})$ . For the A<sub>3</sub> + B<sub>2</sub> system

$$P(F_A^{\text{out}}) = \frac{1 - rp^2}{rp^2} \quad (A1)$$

and for A<sub>4</sub> + B<sub>2</sub>

$$P(F_A^{\text{out}}) = \left[ \frac{1}{rp^2} - \frac{3}{4} \right]^{1/2} - \frac{1}{2} \quad (A2)$$

where  $p$  is the extent of reaction in the A groups and  $rp$  is the extent of reaction in the B groups. For the general A<sub>f</sub> + B<sub>2</sub> copolymerization,  $P(F_B^{\text{out}})$  is related to  $P(F_A^{\text{out}})$  by

$$P(F_B^{\text{out}}) = 1 - \frac{1}{p} [1 - P(F_A^{\text{out}})] \quad (A3)$$

With these quantities, the sol fraction can readily be calculated. For a random A<sub>f</sub> to be part of the sol all  $f$  of its arms must be finite or  $[P(F_A^{\text{out}})]^f$ . Thus for the general A<sub>f</sub> + B<sub>2</sub> copolymerization

$$w_s = w_{A_f}[P(F_{A_f}^{\text{out}})]^f + w_{B_2}[P(F_{B_2}^{\text{out}})]^2 \quad (\text{A4})$$

where  $w_{A_f}$  is the weight fraction of  $A_f$ 's, and  $w_{B_2}$  is the weight fraction of  $B_2$ 's in the starting mixture. For our particular reactants, the first term in eq A4 is always <2% of the second.

For an  $A_f$  group to be a network junction, at least three of its arms must be infinite (connected to the gel). The probability of an arm being infinite is just  $1 - P(F_{A_f}^{\text{out}})$ . Thus the probability that an  $A_f$  group chosen at random is a junction of functionality  $i$  is

$$P(X_i) = \binom{f}{i} [1 - P(F_{A_f}^{\text{out}})]^i [P(F_{A_f}^{\text{out}})]^{f-i} \quad (\text{A5})$$

where  $\binom{f}{i}$  is the usual notation for the number of combinations of  $f$  things taken  $i$  at a time. The concentration of junctions,  $\mu$ , is just the summation of all the junction probabilities times the initial concentration of cross-linker. Since there is only one type of cross-linker in our systems

$$\mu = [A_f]_0 \sum_{i=3}^f P(X_i) \quad (\text{A6})$$

Each end of a network chain must terminate at a junction. Thus, the concentration of network junctions becomes

$$\nu = [A_f]_0 \sum_{i=3}^f \frac{i}{2} P(X_i) \quad (\text{A7})$$

With eq A6 and A7 the modulus for the phantom network, eq 8, or Flory's model, eq 12, can be evaluated. To calculate  $G$  with Langley's trapped entanglement model, we need the trapping factor,  $T_e$ . Langley proposed that an entanglement interaction can be represented by one network chain looping around another. A more general approach is to consider entanglements as pairwise geometrical interactions. From either viewpoint, these interactions will be permanently trapped if all four chain ends leading away from the interaction go to the infinite network. In our  $A_f + B_2$  system, the  $B_2$ 's are involved in the entanglements, and the functionality of the entanglement junctions is 4. Thus

$$P(X_e) = [1 - P(F_{B_2}^{\text{out}})]^4 = T_e \quad (\text{A8})$$

Relations for the weight fraction of pendant material in a network have been derived by Miller, Valles, and Ma-

cosko.<sup>29</sup> For our system with such small  $A_f$  molecules, their eq 6.4 reduces to

$$w_p \simeq 2w_{B_2}P(F_{B_2}^{\text{out}})[1 - P(F_{B_2}^{\text{out}})] \quad (\text{A9})$$

## References and Notes

- (1) Universidad del Sur, Bahia Blanca, Argentina.
- (2) E. M. Valles and C. W. Macosko, *Macromolecules*, **12**, 521 (1979).
- (3) E. M. Valles and C. W. Macosko, *Rubber Chem. Technol.*, **49**, 1232 (1976).
- (4) E. M. Valles and C. W. Macosko in "Networks: Structure and Properties", S. S. Labana, Ed., Academic Press, New York, 1977, p 401.
- (5) E. M. Valles, Ph.D. Thesis, Department of Chemical Engineering and Materials Science, University of Minnesota, Minneapolis, Minn., 1978.
- (6) R. S. Rivlin in "Rheology", Vol. I, F. R. Eirich, Ed., Academic Press, New York, 1956, Chapter 10, p 351.
- (7) P. J. Flory, "Principles of Polymer Chemistry", Cornell University Press, Ithaca, N.Y., 1953.
- (8) L. R. G. Treloar, "The Physics of Rubber Elasticity", 3rd ed., Oxford University Press (Clarendon), London, 1975.
- (9) K. Dusek and W. Prins, *Adv. Polym. Sci.*, **6**, 1 (1969).
- (10) T. L. Smith, *Treatise Mater. Sci. Technol.*, **10**, 369 (1977).
- (11) W. W. Graessley, *Macromolecules*, **8**, 186 (1975).
- (12) D. S. Pearson and W. W. Graessley, *Macromolecules*, **11**, 528 (1978).
- (13) P. J. Flory, *Proc. R. Soc. London, Ser. A*, **351**, 351 (1976).
- (14) D. R. Miller and C. W. Macosko, *Macromolecules*, **9**, 206 (1976).
- (15) W. W. Graessley, *Adv. Polym. Sci.*, **16**, 1 (1974).
- (16) N. R. Langley and K. E. Polmanteer, *J. Polym. Sci., Polym. Phys. Ed.*, **12**, 1023 (1974).
- (17) D. S. Pearson, B. J. Skutnik, and G. G. A. Böhm, *J. Polym. Sci., Polym. Phys. Ed.*, **12**, 925 (1974).
- (18) G. Allen, P. L. Egerton, and D. J. Walsh, *Polymer*, **17**, 65 (1976).
- (19) L. M. Dossin, D. S. Pearson, and W. W. Graessley, *Polym. Prepr., Am. Chem. Soc., Div. Polym. Chem.*, **38**, 224 (1979); *Macromolecules*, **12**, 123 (1979).
- (20) J. E. Mark, *Rubber Chem. Technol.*, **48**, 495 (1975).
- (21) P. J. Flory, *J. Chem. Phys.*, **66**, 5720 (1977).
- (22) N. R. Langley, *Macromolecules*, **1**, 348 (1968).
- (23) C. W. Macosko and W. M. Davis, *Rheol. Acta*, **13**, 814 (1974).
- (24) J. D. Ferry, "Viscoelastic Properties of Polymers", 2nd ed., Wiley, New York, 1970.
- (25) E. A. Collins, J. Bares, and F. W. Billmeyer, "Experiments in Polymer Science", Wiley, New York, 1973.
- (26) M. Gottlieb, personal communication, 1978.
- (27) D. J. Plazek, W. Dannhauser, and J. D. Ferry, *J. Colloid Sci.*, **16**, 101 (1961).
- (28) N. R. Langley and J. D. Ferry, *Macromolecules*, **1**, 353 (1968).
- (29) D. R. Miller, E. M. Valles, and C. W. Macosko, *Polym. Eng. Sci.*, **19**, 272 (1979).
- (30) Y. Isono, T. Fujimoto, N. Takeno, H. Kjiura, and M. Nagasawa, *Macromolecules*, **11**, 888 (1978).
- (31) P. J. Flory and Y. Tatara, *J. Polym. Sci.*, **13**, 683 (1975).
- (32) J. D. Ferry and H.-C. Kan, *Rubber Chem. Technol.*, **51**, 731 (1978).